HHS Public Access

Author manuscript

Biomaterials. Author manuscript; available in PMC 2022 February 01.

Published in final edited form as:

Biomaterials. 2021 February ; 269: 120630. doi:10.1016/j.biomaterials.2020.120630.

A dual-modal PET/near infrared fluorescent nanotag for long-term immune cell tracking

Stefan Harmsen[a,b,#], **Emin Ilker Medine**[a,#], **Maxim Moroz**[a,#], **Fuad Nurili**[c], **Jose Lobo**[a], **Yiyu Dong**[d], **Mezruh Turkekul**[e], **Naga Vara Kishore Pillarsetty**[a], **Richard Ting**[c], **Vladimir Ponomarev**[a,f], **Oguz Akin**[a], **Omer Aras**[a,*]

[a]Department of Radiology, Memorial Sloan Kettering Cancer Center, New York, NY 10065, United States

[b]Department of Pediatrics, Stanford University, Stanford, CA 94305, United States

[c]Molecular Imaging Innovations Institute (MI3), Department of Radiology, Weill Cornell Medical College, New York, NY 10065, United States

[d]Human Oncology and Pathogenesis Program (HOPP), Memorial Sloan Kettering Cancer Center, New York, NY 10065, United States

[e]Molecular Cytology Core Facility, Memorial Sloan Kettering Cancer Center, New York, NY, 10065, United States

[f]Molecular Pharmacology and Chemistry Program, Memorial Sloan Kettering Cancer Center, New York, NY 10065, United States

Abstract

Adoptive cell transfer of targeted chimeric antigen receptor (CAR) T cells has emerged as a highly promising cancer therapy. Their pharmacodynamic action is closely related to their pharmacokinetic profile, because of this as well as risk of non-specific action, it is important to monitor their biodistribution and fate following infusion. To this end, we developed a dual-modal PET/near infrared fluorescent (NIRF) nanoparticle-based imaging agent as non-genomic labels for human CAR T cells. Since the PET/NIRF nanoparticles did not affect cell viability or their cytotoxic functionality, this platform enabled long-term whole-body CAR T cell tracking using

[*]Correspondence should be addressed to: Omer Aras, MD, 300 East 66th Street, New York NY 10065, Phone: +1 646 888 4690, araso@mskcc.org.

Author Contributions

SH, EIM, MM, and OAr designed and performed all experiments, and wrote the manuscript. NVKP assisted in the radiolabeling and characterization of the PET/NIRF nanoparticles. JL isolated and transduced the T cells. FN, EIM, JL labeled the CAR T cells with PET/NIRF nanoparticles. RT and YD performed part of the in vivo experiments. VP, OAk, and OAr supervised the project and coordinated all researchers. All authors have reviewed and approved the manuscript.

[#]These authors contributed equally

Competing Financial Interests: The authors declare no competing financial interests with this publication and there has been no significant financial support for this work that could have influenced its outcome.

PET and NIRF in an ovarian peritoneal carcinomatosis model and is a viable imaging technology to be applied in other cancer models.

Keywords

Dual-modal; PET; near-infrared fluorescence; immune cell labeling; nanomedicine; tracking

INTRODUCTION

Immunotherapy has emerged as a powerful addition to the cancer armamentarium. Immunotherapy is based on treating cancer patients with therapies that activate or uses immune system components to harness their disease. Such immunotherapies can consist of antibodies that block important immunomodulatory proteins that are expressed by cancer cells [1], or may include cancer vaccines [2, 3] or adoptive cell transfer of lymphocytes [4]. In particular, chimeric antigen receptor (CAR) T cell targeting CD19 has shown significant benefit in patients with hematological cancers of B cell lineage and has been approved for the treatment of refractory pre-B cell acute lymphoblastic leukemia and diffuse large B cell lymphoma[5-7]. While targeting of the B cell lineage restricted antigen CD19 has shown great promise, so far the success of CAR-T cell therapy beyond hematological cancers has been limited. Important reasons for the limited success of CAR-T cell targeting of tumor-associated antigens in solid tumors are: tumors are often heterogeneous; immune checkpoints expressed in the tumor microenvironment compromise CAR-T cell tumor penetration; and tumor-associated antigen expression is not restricted to the tumor, leading to off-tumor toxicities such as, but not limited to cerebral edema [8-10].

To understand and address the limitations of CAR-T cells and adoptive cell transfer, in general, as solid tumor therapy, we developed a strategy to enable whole-body, spatiotemporal cell tracking to gain insight into the distribution of adoptively transferred cells. We employed a dual-modal positron emission tomography (PET) and near infrared fluorescence (NIRF) nanoparticle-based direct, non-genomic labeling strategy to monitor T cell distribution following transplantation in tumor-bearing mice (Fig. 1). Typically, in a preclinical setting genomic labeling is employed, in which a reporter gene/protein is introduced in the cells that can be used to detect or track the labeled cells [11]. However, in a clinical setting genomic labeling is not an option. To address this limitation, Thu *et al.* have developed a non-genomic labeling strategy in which protamine and heparin are used to label cells with ferumoxytol – a nanoparticle-based MRI imaging agent with low sensitivity (*i.e.* millimolar range) [12]. Therefore to allow more sensitive imaging, we designed a non-genomic strategy in which we label the cells with a PET/NIRF-active nanotag to offer highly sensitive, whole-body imaging based on PET and additionally enables both highly sensitive, wide-field imaging as well as high-resolution microscopic NIRF imaging. To this end, biocompatible NIRF silica nanoparticles ($\lambda_{ex/em}$: 680/700nm) were intrinsically radiolabeled with ^{89}Zr – clinically approved and widely used positron emitter with a half-life of 78.4 hours[13, 14] – to accommodate long-term PET-based cell tracking. CAR T cells were labeled with the ^{89}Zr-labeled NIR fluorescent silica nanoparticles *ex vivo* using a heparin- and protamine-based cell labeling prior to transplantation[12, 15]. In this paper, we

demonstrate that our strategy of using a dual-modal PET/NIRF nanotag to track adoptively transferred immune cells was successful for enabling long-term cell tracking as well as interrogating the cellular fate and tissue distribution of adoptively transferred immune cells.

MATERIALS AND METHODS

Chemicals

All reagents were obtained from Sigma Aldrich (St. Louis, MO) and used without any further purification. ^{89}Zr ($t_{1/2}$=78.4 h) was produced at Memorial Sloan Kettering Cancer Center (New York, NY) on a TR19/9 cyclotron (Ebco Industries Inc., Vancouver, BC) via the ^{89}Y(p,n) ^{89}Zr reaction and purified to yield [^{89}Zr]-zirconium oxalate[16].

Nanoparticle synthesis and characterization

NIRF silica nanoparticle synthesis: CF680R (1 μmole, Biotium Inc., Fremont, CA) was reacted overnight with 0.4 μl 3-(mercaptopropyl)trimethoxysilane (MPTMS) in dimethylformamide (DMF; 100 μL) to yield CF680R-MPTMS. CF680R-MPMTS (4 μL 10 mM in DMF) was added without purification to a solution of 40 ml isopropanol containing 2.5 ml tetraethyl orthosilicate (TEOS; 99.99% purity), 3.5 mL water, and 1.5 mL ammonium hydroxide (28%). The solution was stirred for 15 min and NIRF silica nanoparticles were collected via centrifugation (10,000 *g*; 10 min) and washed with ethanol. The NIRF nanoparticles were redispersed in 10 mM 2-(*N*-morpholino)ethanesulfonic acid (MES) buffer (pH 7.3) at a concentration of 10 nM.

^{89}Zr-labeling of NIRF silica nanoparticles: ^{89}Zr-oxalate (1.3 mCi) was neutralized with 1.0 M sodium carbonate and added to a 100 μL dispersion of NIRF silica nanoparticles (10 nM) in 10 mM MES buffer (pH 7.3). After 30 min at 70 °C, the reaction mixture was centrifuged at 10,000 *g* for 10 min and the supernatant was removed to rid any free ^{89}Zr. The dual-modal PET/NIRF nanotags were redispersed in water (18 MΩ·cm) at a concentration of 10 nM.

PET/NIRF nanotag characterization: Before radiolabeling, transmission electron micrographs were obtained of the NIRF nanoparticles using a JEOL 1200ex-II operated at 80keV and the hydrodynamic size distribution and the concentration of the NIRF nanoparticles were measured using a nanoparticle tracking analyzer (NTA; NS300, Malvern Instruments, Malvern, UK). The radiolabeling yield of the PET/NIRF nanotags was calculated using the instant thin layer radio-chromatography (iTLC) method. Diethylenetriaminepentaacetic acid (DTPA; 5 mM; pH 5) solution was used as the mobile phase. Following iTLC, the plates were counted using a Bioscan AR-2000 Radio-TLC Imaging Scanner (Eckert & Ziegler Radiopharma, Berlin, Germany).

In vitro cell-labeling and adoptive transfer

CAR T cell labeling with dual-modal PET/NIRF nanotags: The dual-modal PET/NIRF nanotags (200 μl 10 nM) were redispersed in 600 μl of serum-free RPMI 1640 cell media (Corning, Manassas, VA) supplemented with 40 μg/ml of protamine sulfate (10 mg/ml ; Fresenius Kabi, Lake Zurich, IL) and 2U/ml of heparin (10 U/ml; Fresenius Kabi, Lake

Zurich, IL) and vortexed for 2 min. Human carcinoembryonic antigen (hCEA)-redirected CAR T cells were kindly provided by the Ponomarev Lab at Memorial Sloan Kettering Cancer Center. hCEA-CAR T cells (2×10^6 cells) suspended in serum-free RPMI (200 μl) were added to the protamine sulfate-heparin complexed PET/NIRF nanotag dispersion and incubated for 30 min at 37 °C. After 1 h incubation, the PET/NIRF nanotag-labeled CAR T cells were washed twice with serum-free RMPI media. The amounts of radioactivity associated with the cells before and after the labeling procedure were determined using a CRC-55tR dose calibrator (Capintac Inc., Florham Park, NJ). Cell viability was assessed using a trypan blue exclusion test.

CAR T Cell viability: Cell viability was assessed in PET/NIRF nanotag-labeled CAR T cells and compared to viability of unlabeled CAR T cells. Cells were suspended in 1× PBS at a concentration of 1×10^6/ml and mixed with 0.4% of trypan blue dye at a 1:1 ratio. Ten μl of this mixture was used to count the alive and dead cells either manually by a hemocytometer or automatically by Countess Automated Cell Counter (Invitrogen Corp., Carlsbad, CA). Cells with an intact membrane excluded the dye and were considered as live cells. The percentage of viable cells was determined.

PET/NIRF nanotag post-labeling retention: PET/NIRF nanotag-labeled CAR T cells were seeded (10^5 cells/well) in a clear-bottom black 96-well plate. At day 1, 4, 7, the supernatant was transferred to an empty well and near-infrared fluorescence intensity of CAR T cell- and supernatant containing wells were measured on an Odyssey Near-Infrared Fluorescence Imaging System (LI-COR Biosciences, Lincoln, NB).

***In vivo* studies—**All animal studies were performed under a Memorial Sloan Kettering Cancer Center protocol #05-07-012 approved by the Institutional Animal Care and Use Committee.

Cell tracking of adoptively transferred PET/NIRF nanotag-labeled CAR T cells: Female NOD/SCID *Il2rg*$^{-/-}$ (NSG) mice (5–6 weeks of age) were obtained from The Jackson Laboratory (Bar Harbor, ME) and these tumor-naïve animals were randomly divided into two groups (n=5/group) and injected intravenously (i.v.) or intraperitoneally (i.p.) with 1×10^6 PET/NIRF nanotag-labeled CAR T cells, respectively. The spatiotemporal distribution of the PET/NIRF nanotag-labeled CAR T cells was monitored using microPET imaging (Focus 120; Siemens Medical Solutions USA, Inc.) over the course of 14 days post injection (p.i.). During each session a background scan and an image of the standard were also acquired. With the exception of the background, a minimum of 15×10^6 true counts per scan were collected to ensure adequate image quality. This required acquisition times of 5 min (day 0 p.i.), 5 min (day 1 p.i.), 15 min (day 7 p.i.), and 20 min (day 14 p.i.). The mice were anesthetized during image acquisition using isoflurane (Forane; Baxter). PET images were registered and reconstructed using ASIPro image-display software (Siemens Medical Solutions USA, Inc.). After the final scan at day 14 p.i., the animals were sacrificed, and the major organs were harvested. NIRF imaging of the organs was performed on an Odyssey Imaging System (LI-COR Biosciences, Lincoln, NB).

Adoptive cell transfer in an intraperitoneal carcinomatosis animal model: Female NOD/SCID *Il2rg*$^{-/-}$ (NSG) mice (n=5) were injected intraperitoneally (i.p.) with 1 × 10^6 SKOV3:hCEA(+) cells (kindly provided by the Ponomarev Lab at Memorial Sloan Kettering Cancer Center) in 150 μL RPMI 1640. Tumor growth was monitored using bioluminescent imaging (BLI). Bioluminescence images were collected in a Xenogen IVIS Imaging System. For imaging tumor cells, a single retro-orbital (RO) injection of 150 mg/kg D-luciferin (Gold Biotechnology, St. Louis) in PBS was administered to each mouse 10–15 mins before imaging, on the first day of injected labeled T cells. For imaging T cells, similarly we administered bolus RO injection with 10 μg of coelenterazine (Nanolight Technology) 10–15 s before imaging, on the second day of labeled T cells. We imaged the mice individually when coelenterazine substrate was used. Two weeks following intraperitoneal administration of SKOV3;hCEA(+), PET/NIRF nanotag-labeled hCEA-redirected CAR T cells (20 × 10^6 cells) were adoptively transferred via intraperitoneal administration. Distribution of PET/NIRF nanotag-labeled CAR T cells over time was assessed via PET, BLI, and optical imaging. At 15 days (~5 half-lives of ^{89}Zr), animals were sacrificed and the carcasses were processed for histopathological assessment and multiplex immunofluorescence microscopy.

Histology: The carcasses were fixed in 4% paraformaldehyde and processed for paraffin embedding using Leica ASP6025 tissue processor (Leica Biosystems, Buffalo Grove, IL). Freshly cut 5 micron paraffin sections of the peritoneal cavity were stained for sequential double immunofluorescence on Leica Bond RX (Leica Biosystems, Buffalo Grove, IL) with 0.6 ug/ml CD3 Rabbit Polyclonal (Dako cat#A0452, Santa Clara, CA) for 1 hour and using 10 min of 1:200 Tyramide Alexa Fluor488 detection (Life Technologies, Gaithersburg, MD) on Protocol F, followed by 4 ug/ml hCEA Rabbit Monoclonal (Abcam cat#15987, Cambridge, MA) for 1 hour and using 10 min of 1:200 Tyramide Alexa Fluor568 detection (Life Technologies, Gaithersburg, MD) on Protocol F. The sections were pre-treated with Leica Bond ER2 Buffer (Leica Biosystems, Buffalo Grove, IL) for 20 min at 100°C before each staining. After staining the sections were dehydrated and mounted with Permount for digital scanning with Pannoramic Confocal (3DHistech, Budapest, Hungary) using 40X water objective.

RESULTS

Synthesis and radiolabeling of near-infrared fluorescent silica nanoparticles

The synthesis of the NIRF silica nanoparticles was a two-step process. First, we produced silane-appended CF680R (CF-MPTMS) by reacting CF680R-maleimide with 3-mercaptopropyltrimethoxysilane (MPTMS). Then, the silane-appended dye (CF680R-MPTMS) was used without further purification to synthesize the NIRF nanoparticles using a modified Stöber method[17]. As shown in Fig. 2, the NIRF nanoparticles had a mean hydrodynamic diameter of 120 nm and a limit of detection of ~70 fM as measured on an Odyssey Imaging System (LI-COR Biosciences, Lincoln, NE). The NIRF nanoparticles were labeled with neutralized ^{89}Zr using our previously reported chelator-free radiolabeling protocol[13] affording dual-modal PET/NIRF nanotags. The ^{89}Zr-radiolabeling efficiency of the NIRF silica nanoparticles was determined to be >98% based on instant thin layer chromatography (iTLC; Fig. 2c), which was similar to the previously reported efficiency for

radiolabeling of non-fluorescent silica nanoparticles[13]. Of note, all radioactivity was associated with the PET/NIRF nanotags and no free ^{89}Zr was present in the aqueous PET/NIRF nanotag dispersion after washing (Fig. 2c). We determined that on average 1525 ^{89}Zr isotopes were associated with one NIRF nanotag.

Ex vivo CAR T cell labeling with PET/NIRF nanotags

As shown in Fig. 3, CAR T cell labeling with PET/NIRF nanotags was markedly improved when performed in the presence of protamine and heparin. Using a dose calibrator, it was determined that the cell labeling yield of the CAR T cells with PET/NIRF nanoparticles was 82.6% (±5.1) with a cell viability of >90%. We found that the PET/NIRF nanotags were retained by the CAR T cells up to 7 days post labeling (Fig. 3e-f). As shown in Movie 1, when co-cultured with CEA-overexpressing SKOV3 cells, the PET/NIRF nanotag-labeled CAR T cells retained their functional activity and were able to induce apoptosis of the CEA-overexpressing SKOV3 cells *in vitro*.

Cell tracking of PET/NIRF nanotag-labeled CAR T cells in naïve animals

Next, we studied the feasibility of using PET/NIRF nanotag-labeled CAR T cells for long-term cell tracking and biodistribution studies following different routes of administration. The PET/NIRF nanotag-labeled CAR T cells (20×10^6 cells) were adoptively transferred to naïve wild-type NSG mice (n=5) via either an intravenous or an intraperitoneal route of administration. PET imaging demonstrated that the intravenously injected PET/NIRF nanotag-labeled cells distributed mostly to the lungs and liver, while the intraperitoneally administered cells distributed to liver and spleen (Fig. 4a, b). Interestingly, it was observed that within 3 days following i.p. administration of the nanotag-labeled CAR T cells, the PET signal from the intraperitoneal cavity in these tumor-naïve animals completely disappeared and mostly focused in the liver and spleen. Of note, both routes of administration resulted in background signal in the bones (t>3 days). Immunohistochemical examination of the bone marrow demonstrated the presence of human $CD3^+$ T cells (Fig. 4c). Furthermore, while unchelated Zr^{4+}-ions are known for their high osteophilicity, in a previous study we have shown that silica nanoparticles bind Zr^{4+} with high affinity and we found no evidence of any bone uptake as a result of dissociated $^{89}Zr^{4+}$ following intravenous injection of ^{89}Zr-labeled silica nanoparticles[13]. After 14 days (approximately 5 half-lives of ^{89}Zr), the animals were sacrificed and endpoint NIRF imaging showed a good correlation between PET imaging and NIRF imaging. The endpoint NIRF signal was associated with the lungs and liver and with the liver and spleen following intravenous and intraperitoneal administration, respectively.

Cell tracking of PET/NIRF nanotag-labeled CAR T cells in a mouse model of peritoneal carcinomatosis

Intraperitoneal administration proved to be a viable route for adoptive transfer of the NIRF/PET nanotag-labeled hCEA-redirected CAR T cells in animals bearing peritoneal tumor deposits of hCEA-overexpressing SKOV3 cells. As shown in Figure 5, 1 day following adoptive transfer of the CAR T cells, the BLI signal of SKOV3:hCEA(+) (Fig. 5a) and CAR T cells were overlapping, particularly in the lesion indicated by the arrowhead (Fig 5a, b; day 1). At 1 week post PET/NIRF nanotag-labeled CAR T cells administration, the BLI of the CAR T cells and PET image demonstrated marked overlap. Only one hotspot was

present on the PET image, but this did not match with CAR T cell BLI results (Fig. 5b; day 7; lesion 4). Interestingly, at 2 weeks post i.p. administration of PET/NIRF nanotag-labeled CAR T cells, the BLI signal of the CAR T cells was mostly localized to a single focus (Fig. 5b; day 14; lesion 4). As shown in Fig. 5c, the CAR T cells co-localized with a peritoneal lesion of SKOV3:hCEA(+) but were mostly found on the periphery of the tumor.

Of note, the PET image at day 14 showed more overlap with the BLI signal of the CAR T cells at day 7 than at day 14. This discrepancy between BLI and PET imaging could indicate that in the second week post CAR T cell administration, the PET/NIRF nanotags are released from the CAR T cells and deposit at the site of release. This is further corroborated by microscopic imaging of the PET/NIRF nanoparticles using NIRF. As shown in Fig. 5d, at day 14 the PET/NIRF nanotags were no longer associated with the hCEA-redirected CAR T cells, but their signal co-localized with the SKOV3:hCEA(+) cells, indicating that the PET/NIRF nanotags were transported to the tumor deposit, dissociated from the CAR T cells, and co-localized with the tumor cells. This timeframe is in line with our *in vitro* findings (Fig 3e-f) in which we found that the CAR T cells start to release PET/NIRF nanotags around day 7 post labeling.

DISCUSSION

In the current study, we demonstrated the development and feasibility of a dual-modal PET/NIRF nanotag imaging agent that enables straightforward and highly efficient non-genomic cell labeling to study the fate of adoptively transferred CAR T cells using whole-body PET as well as high-resolution near-infrared fluorescence imaging up to 1 week post adoptive transfer.

Non-genomic *ex vivo* labeling of (immune) cells with radionuclides traditionally involved a radiometal (*e.g.* ^{111}In, ^{64}Cu, ^{89}Zr, *etc.*) complexed to a ligand (e.g. oxine, pyruvaldehydebis(N4- methylthiosemicarbazone (PTSM), protamine sulfate, *etc.*) to facilitate active transport of the radiometal complex across the membrane into immune cells[18-21]. However, such approaches markedly affect the functionality and viability of labeled cells, and, in addition, active efflux of radiometals limits labeling efficiency, long-term cell tracking, and reduced signal to background. Therefore, cell labeling strategies were developed that were aimed at *ex vivo* labeling of cell surface proteins using radiolabeled, non-internalizing antibodies or covalent binding of radiometal-chelator complexes[22, 23]. While these strategies generally enabled robust cell labeling, it is unclear whether the (random) modifications of cell surface proteins affects the functionality or immunogenicity of the labeled cell. To mitigate this, Griessinger *et al.* demonstrated an intracellular radiolabeling approach that was based on the internalization of ^{64}Cu-labeled antibodies upon antigen-binding[24]. Using this cell labeling strategy, they showed labeling efficiencies of >97%, cell tracking ability using PET for up to 48 h post adoptive transfer, and, as a result of improved intracellular trapping of the radioisotope they achieved low, unspecific background signals that enabled the use of less activity for quantitative imaging studies. Drawbacks of this approach however are 1) that it relies on antibodies against a certain target; 2) only a limited amount of radioisotopes can be conjugated to the antibody; 3) the antigen has to be

expressed on the target cell; 4) upon binding, the antigen should be internalized and display continuous plasma membrane turnover to achieve sufficient uptake of the radiotracer.

To address these limitations, we developed a strategy that does not rely on the expression of a specific target protein. Our approach is based on the labeling of (immune) cells with nanoparticles as first reported by Thu *et al.* in which they used self-assembling nanocomplexes by combining three FDA-approved drugs – protamine, heparin, and ferumoxytol (superparamagnetic iron oxide nanoparticle (SPION)) – in medium containing cells leading to direct cell labeling for cell tracking and MRI detection[12]. While MRI enables whole-body imaging, it has lower sensitivity relative to PET. We therefore used near-infrared fluorescent nanoparticles that were intrinsically labeled with ^{89}Zr using our previously described nanoparticle radiolabeling protocol to yield a dual-modal PET/NIRF nanotags[13, 14]. By complexing these PET/NIRF nanotags with protamine and heparin in the presence of CAR T cells, this allowed us to directly and efficiently label these cells to achieve sufficient uptake of the radiotracer and enable whole-body cell tracking using PET for up to 1 week following adoptive cell transfer.

Our labeling strategy has been designed to be clinically applicable. In fact, all major reagents are already used in the clinic. Protamine and heparin are FDA-approved, ^{89}Zr is routinely used in immuno-PET imaging, and fluorescent silica nanoparticles have recently successfully been translated to the clinic. The radiation dose of 92 kBq/10^6 CAR T cells did not affect cell viability and efficacy, which is supported by a study of Weist et al. who demonstrated that below 140kBq/10^6 cells no effect on viability and functionality are to be expected [18]. Our immune cell labeling protocol has been designed to seamlessly fit within the workflow for CAR T cell manufacturing directly after the T cell expansion step (Fig. 1) [25] and can be extended to other immune cells such as NK cells as well[26, 27]. In this way, cell-based therapies can be produced via a non-genomic labeling procedure that allow the dynamic monitoring of immune cells for up to 1 week post adoptive transfer, which is within the most critical window for monitoring of engraftment/trafficking.

With a half-life of 78.4 h (3.3d), ^{89}Zr theoretically should enable PET-based cell tracking for up to ~2 weeks post adoptive cell transfer. However, post mortem analysis using near-infrared fluorescence demonstrated that at >1 week post adoptive cell transfer, the dual-modal PET/NIRF nanotags are no longer associated with immune cells. This has been reported for other nanoparticle-based cell-labeling strategies as well. Important underlying reasons for the release of nanoparticle-based imaging agents from labeled cells due to apoptosis[28]. However, while this is regarded as a major drawback of nanoparticle-based labeling agents, we demonstrate using *post mortem* NIRF imaging of a peritoneal tumor section that the released PET/NIRF nanotags are taken up by the tumor cells. Although beyond the scope of the current study, this observation has important implications that we briefly would like to discuss. The use of immune cells as carriers to improve the delivery of nanomedicines to tumors has been previously explored. To achieve high nanoparticle loading efficiencies either 1) phagocytic cells (*e.g.* monocytes or macrophages) were used, but these lack tumor specificity[29], or, 2) tumor specific T cells, which, as a result phagocytosis capabilities, were labeled with nanodrugs through non-specific conjugation to cell surface receptors, which may affect cell functionality, homing, or could induce

immunogenicity[30]. By contrast, our direct T cell labeling approach enabled high nanoparticle loading efficiency (>80%), stable intracellular trapping, efficient tumor homing, and release of the nanotag at the tumor site. In future studies, we would like to address whether we can use our direct cell labeling approach to deliver clinically applied nanomedicines such as Doxil using CAR T, NK, or other immune cells.

In summary, we have developed a clinically translatable PET/NIRF nanotag-based direct immune cell labeling approach that enables whole-body cell tracking for up to 1 week post adoptive cell transfer. Moreover, our approach has the potential to be transformative for immune cell-based nanodrug delivery to improve tumor accumulation of nanomedicines.

Supplementary Material

Refer to Web version on PubMed Central for supplementary material.

Acknowledgments

The authors would like to thank the Electron Microscopy and Molecular Cytology Core Facility at Memorial Sloan Kettering Cancer Center (MSKCC). This work has been financially supported by the Scientific and Technological Research Council of Turkey (TUBİTAK) [BIDEB-2219] Postdoctoral Research program. This research was funded in part through the NIH/NCI Cancer Center Support Grant [P30 CA008748].

Funding Sources: This work has been financially supported by the Scientific and Technological Research Council of Turkey (TUBİTAK) [BIDEB-2219] Postdoctoral Research program. This research was funded in part through the NIH/NCI Cancer Center Support Grant [P30 CA008748]. The funding sources had no involvement in study design; in the collection, analysis and interpretation of data; in the writing of the report; and in the decision to submit the article for publication.

ABBREVIATIONS:

BLI	bioluminescent imaging
CAR	chimeric antigen receptor
iTLC	instant thin layer radio-chromatography
NIRF	near infrared fluorescent
PET	positron emission tomography
RO	retro-orbital
SPION	superparamagnetic iron oxide nanoparticle

REFERENCES

[1]. Wei SC, Duffy CR, Allison JP, Fundamental Mechanisms of Immune Checkpoint Blockade Therapy, Cancer Discov 8(9) (2018) 1069–1086. [PubMed: 30115704]

[2]. Mukalel AJ, Riley RS, Zhang R, Mitchell MJ, Nanoparticles for nucleic acid delivery: Applications in cancer immunotherapy, Cancer Lett 458 (2019) 102–112. [PubMed: 31100411]

[3]. Zhang R, Billingsley MM, Mitchell MJ, Biomaterials for vaccine-based cancer immunotherapy, J Control Release 292 (2018) 256–276. [PubMed: 30312721]

[4]. Rosenberg SA, Restifo NP, Yang JC, Morgan RA, Dudley ME, Adoptive cell transfer: a clinical path to effective cancer immunotherapy, Nat Rev Cancer 8(4) (2008) 299–308. [PubMed: 18354418]

[5]. Brentjens RJ, Davila ML, Riviere I, Park J, Wang X, Cowell LG, Bartido S, Stefanski J, Taylor C, Olszewska M, Borquez-Ojeda O, Qu J, Wasielewska T, He Q, Bernal Y, Rijo IV, Hedvat C, Kobos R, Curran K, Steinherz P, Jurcic J, Rosenblat T, Maslak P, Frattini M, Sadelain M, CD19-targeted T cells rapidly induce molecular remissions in adults with chemotherapy-refractory acute lymphoblastic leukemia, Sci Transl Med 5(177) (2013) 177ra38.

[6]. Neelapu SS, Locke FL, Bartlett NL, Lekakis LJ, Miklos DB, Jacobson CA, Braunschweig I, Oluwole OO, Siddiqi T, Lin Y, Timmerman JM, Stiff PJ, Friedberg JW, Flinn IW, Goy A, Hill BT, Smith MR, Deol A, Farooq U, McSweeney P, Munoz J, Avivi I, Castro JE, Westin JR, Chavez JC, Ghobadi A, Komanduri KV, Levy R, Jacobsen ED, Witzig TE, Reagan P, Bot A, Rossi J, Navale L, Jiang Y, Aycock J, Elias M, Chang D, Wiezorek J, Go WY, Axicabtagene Ciloleucel CAR T-Cell Therapy in Refractory Large B-Cell Lymphoma, New Engl J Med 377(26) (2017) 2531–2544. [PubMed: 29226797]

[7]. Park JH, Riviere I, Gonen M, Wang XY, Senechal B, Curran KJ, Sauter C, Wang YZ, Santomasso B, Mead E, Roshal M, Maslak P, Davila M, Brentjens RJ, Sadelain M, Long-Term Follow-up of CD19 CAR Therapy in Acute Lymphoblastic Leukemia, New Engl J Med 378(5) (2018) 449–459. [PubMed: 29385376]

[8]. Slaney CY, Kershaw MH, Darcy PK, Trafficking of T Cells into Tumors, Cancer Res 74(24) (2014) 7168–7174. [PubMed: 25477332]

[9]. Newick K, Moon E, Albelda SM, Chimeric antigen receptor T-cell therapy for solid tumors, Mol Ther-Oncolytics 3 (2016).

[10]. Bonifant CL, Jackson HJ, Brentjens RJ, Curran KJ, Toxicity and management in CAR T-cell therapy, Mol Ther-Oncolytics 3 (2016).

[11]. Jurgielewicz P, Harmsen S, Wei E, Bachmann MH, Ting R, Aras O, New imaging probes to track cell fate: reporter genes in stem cell research, Cell Mol Life Sci 74(24) (2017) 4455–4469. [PubMed: 28674728]

[12]. Thu MS, Bryant LH, Coppola T, Jordan EK, Budde MD, Lewis BK, Chaudhry A, Ren J, Varma NR, Arbab AS, Frank JA, Self-assembling nanocomplexes by combining ferumoxytol, heparin and protamine for cell tracking by magnetic resonance imaging, Nat Med 18(3) (2012) 463–7. [PubMed: 22366951]

[13]. Shaffer TM, Wall MA, Harmsen S, Longo VA, Drain CM, Kircher MF, Grimm J, Silica nanoparticles as substrates for chelator-free labeling of oxophilic radioisotopes, Nano Lett 15(2) (2015) 864–8. [PubMed: 25559467]

[14]. Shaffer TM, Harmsen S, Khwaja E, Kircher MF, Drain CM, Grimm J, Stable Radiolabeling of Sulfur-Functionalized Silica Nanoparticles with Copper-64, Nano Lett 16(9) (2016) 5601–4. [PubMed: 27464258]

[15]. Pantin JM, Hoyt RF, Aras O, Sato N, Chen MY, Hunt T, Clevenger R, Eclarinal P, Adler S, Choyke P, Childs RW, Optimization of Intrabone Delivery of Hematopoietic Progenitor Cells in a Swine Model Using Cell Radiolabeling with [89]zirconium, Am J Transplant 15(3) (2015) 606–617. [PubMed: 25656824]

[16]. Holland JP, Sheh Y, Lewis JS, Standardized methods for the production of high specific-activity zirconium-89, Nucl Med Biol 36(7) (2009) 729–39. [PubMed: 19720285]

[17]. Stober W, Fink A, Bohn E, Controlled Growth of Monodisperse Silica Spheres in Micron Size Range, J Colloid Interf Sci 26(1) (1968) 62-&.

[18]. Weist MR, Starr R, Aguilar B, Chea J, Miles JK, Poku E, Gerdts E, Yang X, Priceman SJ, Forman SJ, Colcher D, Brown CE, Shively JE, PET of Adoptively Transferred Chimeric Antigen Receptor T Cells with (89)Zr-Oxine, J Nucl Med 59(10) (2018) 1531–1537. [PubMed: 29728514]

[19]. Sato N, Wu H, Asiedu KO, Szajek LP, Griffiths GL, Choyke PL, (89)Zr-Oxine Complex PET Cell Imaging in Monitoring Cell-based Therapies, Radiology 275(2) (2015) 490–500. [PubMed: 25706654]

[20]. Man F, Lim L, Shmeeda H, Gabizon A, Blower P, Fruhwirth G, de Rosales RTM, Direct Cell Labelling with Zr-89(oxine)(4) allows In Vivo PET Imaging of Gamma-delta T-cells in a Breast Cancer Model, Journal of Nuclear Medicine 58 (2017).

[21]. Adonai N, Adonai N, Nguyen KN, Walsh J, Iyer M, Toyokuni T, Phelps ME, McCarthy T, McCarthy DW, Gambhir SS, Ex vivo cell labeling with 64Cu-pyruvaldehydebis(N4-methylthiosemicarbazone) for imaging cell trafficking in mice with positron-emission tomography, Proc Natl Acad Sci U S A 99(5) (2002) 3030–5. [PubMed: 11867752]

[22]. Tarantal AF, Lee CC, Kukis DL, Cherry SR, Radiolabeling human peripheral blood stem cells for positron emission tomography (PET) imaging in young rhesus monkeys, PLoS One 8(10) (2013) e77148. [PubMed: 24098579]

[23]. Bansal A, Pandey MK, Demirhan YE, Nesbitt JJ, Crespo-Diaz RJ, Terzic A, Behfar A, DeGrado TR, Novel Zr-89 cell labeling approach for PET-based cell trafficking studies, Ejnmmi Res 5 (2015).

[24]. Griessinger CM, Maurer A, Kesenheimer C, Kehlbach R, Reischl G, Ehrlichmann W, Bukala D, Harant M, Cay F, Bruck J, Nordin R, Kohlhofer U, Rammensee HG, Quintanilla-Martinez L, Schaller M, Rocken M, Pichler BJ, Kneilling M, 64Cu antibody-targeting of the T-cell receptor and subsequent internalization enables in vivo tracking of lymphocytes by PET, Proc Natl Acad Sci U S A 112(4) (2015) 1161–6. [PubMed: 25587131]

[25]. Wang XY, Riviere I, Clinical manufacturing of CAR T cells: foundation of a promising therapy, Mol Ther-Oncolytics 3 (2016).

[26]. Li KA, Gordon AC, Zheng LF, Li WG, Guo Y, Sun J, Zhang GX, Han GH, Larson AC, Zhang ZL, Clinically applicable magnetic-labeling of natural killer cells for MRI of transcatheter delivery to liver tumors: preclinical validation for clinical translation, Nanomedicine-Uk 10(11) (2015) 1761–1774.

[27]. Su ZL, Wang XF, Zheng LF, Lyu TC, Figini M, Wang B, Procissi D, Shangguan JJ, Sun C, Pan L, Qin L, Zhang B, Velichko Y, Salem R, Yaghmai V, Larson AC, Zhang ZL, MRI-guided interventional natural killer cell delivery for liver tumor treatment, Cancer Med-Us 7(5) (2018) 1860–1869.

[28]. Wang PC, Shan L, Essential Elements to Consider for MRI Cell Tracking Studies with Iron Oxide-based Labeling Agents, J Basic Clin Med 1(1) (2012) 1–6. [PubMed: 24159426]

[29]. Choi MR, Stanton-Maxey KJ, Stanley JK, Levin CS, Bardhan R, Akin D, Badve S, Sturgis J, Robinson JP, Bashir R, Halas NJ, Clare SE, A cellular Trojan Horse for delivery of therapeutic nanoparticles into tumors, Nano Lett 7(12) (2007) 3759–65. [PubMed: 17979310]

[30]. Huang BN, Abraham WD, Zheng YR, Lopez SCB, Luo SS, Irvine DJ, Active targeting of chemotherapy to disseminated tumors using nanoparticle-carrying T cells, Science Translational Medicine 7(291) (2015).

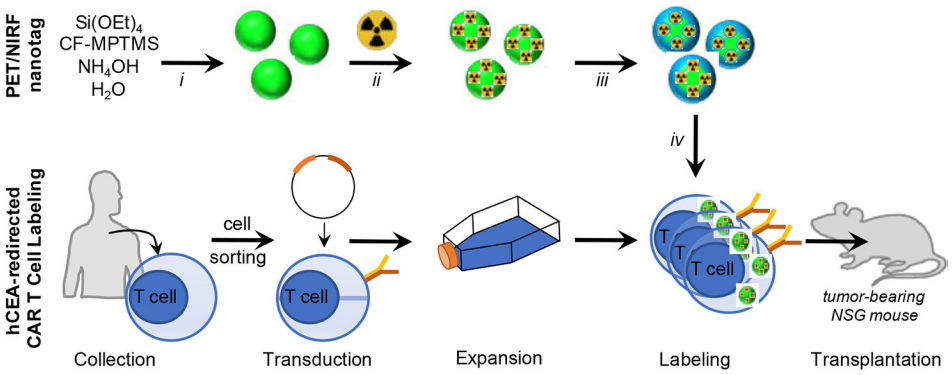

Figure 1. Experimental design.

Near infrared fluorescent (NIRF) silica nanoparticles are synthesized using a Stöber method containing the silane-appended near-infrared fluorophore (CF-MPTMS) and radiolabeled with ^{89}Zr (*ii*) to yield dual-modal PET/NIRF nanotags, which are coated with protamine and heparin (*iii*) to facilitate chimeric antigen receptor (CAR) T cell labeling (*iv*). The PET/NIRF nanotag-labeled hCEA-redirected CAR T cells are transplanted into tumor-bearing subjects. Reaction conditions: *i*. isopropanol, 30 min; *ii*. ^{89}Zr-oxalate (pH 7), 30 min, 70 °C; *iii*. Protamine (40 μg/ml), heparin (2 IU/ml); *iv*. 60 min, 37 °C.

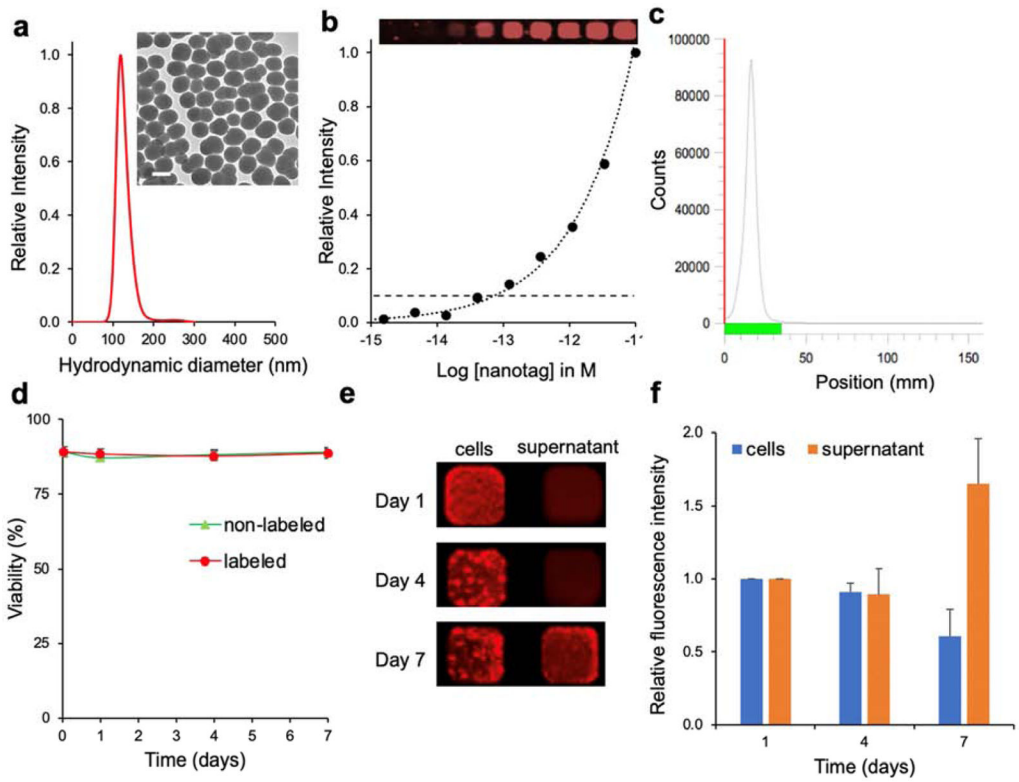

Figure 2. Characterization of PET/NIRF nanotags.

a, Nanoparticle tracking analysis (NTA) and transmission electron microscopy (inset; scale bar, 100 nm) of unlabeled NIRF nanoparticles. **b,** Detection limit of NIRF nanoparticles (inset; actual NIRF image) of dilution curve in 384-well plate. **c,** Instant thin layer chromatography (iTLC) of PET/NIRF nanoparticles after radiolabeling demonstrates that all ^{89}Zr is chelated to the NIRF nanoparticle and no free ^{89}Zr ions are present in the dispersion. **d,** CAR T cell viability of cells labeled with the PET/NIRF nanotag (labeled) and without labeling (non-labeled). **e,f,** Near-infrared fluorescence intensity of PET/NIRF nanotag-labeled CAR T cells and respective supernatants at days 1, 4, and 7 post labeling. The data represent the mean±standard deviation (n=3).

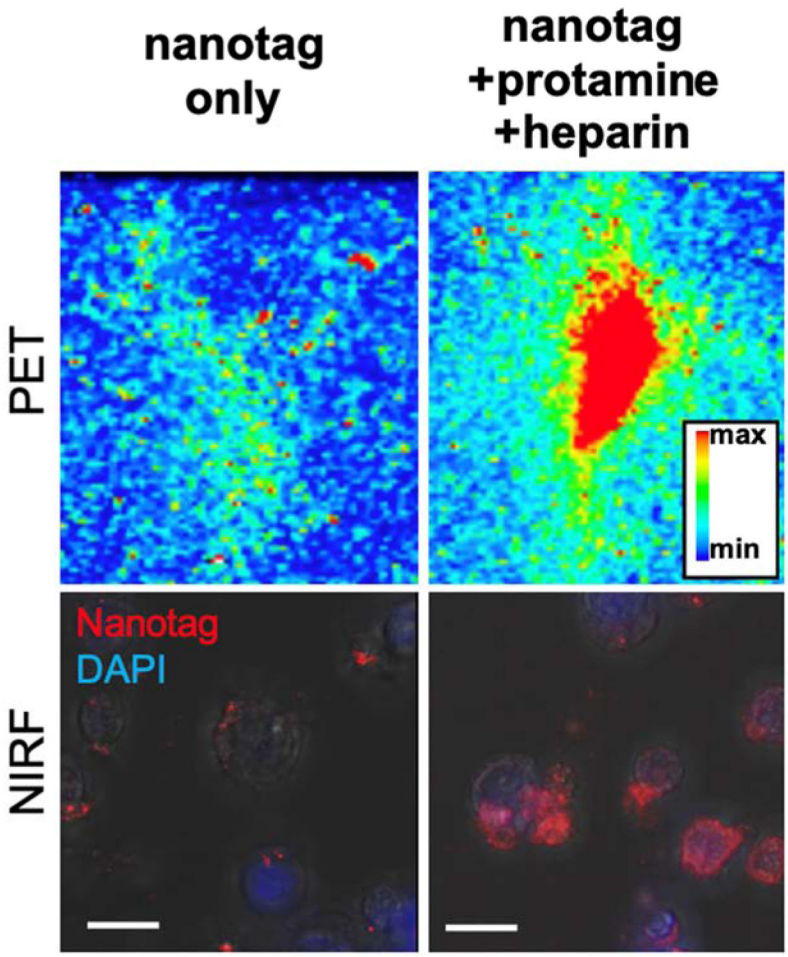

Figure 3. CAR T cell PET/NIRF nanotag labeling.

CAR T cells (10×10^6 cells) were labeled with nanotags alone or in the presence of protamine/heparin. PET imaging of a vial containing the cells was performed at 6 h post PET/NIRF nanotag labeling. NIRF imaging was performed on labeled cells that were seeded, grown, and fixed in a 6 well plate. Cells were stained with DAPI and fluorescence microscopy was performed to image DAPI and the PET/NIRF nanotags.

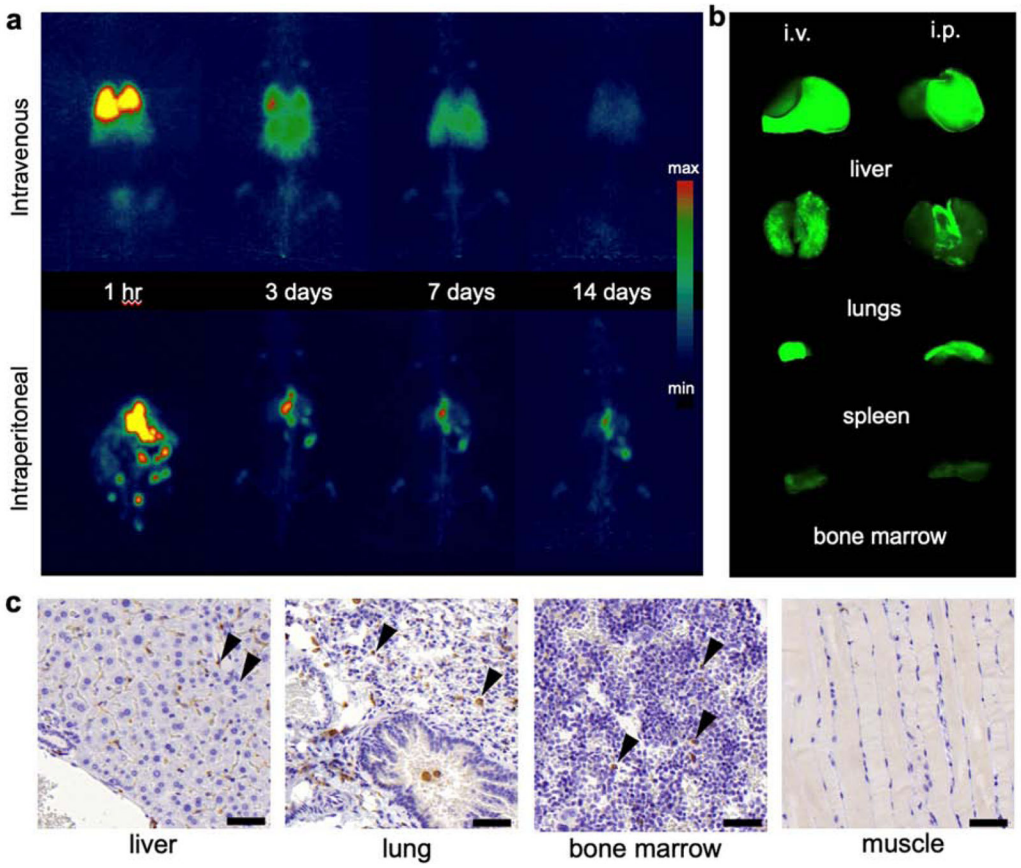

Figure 4. Biodistribution of PET/NIRF nanoparticle-labeled T cells.

a, Coronal PET maximal intensity projections (MIP) at the indicated time points post injection (p.i.) of intravenously (i.v.; top panel) or intraperitoneally (i.p.; bottom panel) infused PET/NIRF nanotag-labeled hCEA-redirected CAR T cells (1.85 MBq; 20×10^6 cells/mice) in tumor-naïve NSG mice (n=5). b, Near-infrared fluorescence imaging of the indicated organs at t=14 days p.i. following adoptive transfer (i.v. or i.p.) of the PET/NIRF nanotag-labeled hCEA-redirected CAR T cells. **c,** Immunohistochemistry staining of CD3 (arrow heads) in the liver, lungs, bone marrow, and muscle (negative control) of a mouse that received PET/NIRF nanotag-labeled hCEA-directed CAR T cells (i.p.). Scale bar, 50 μm.

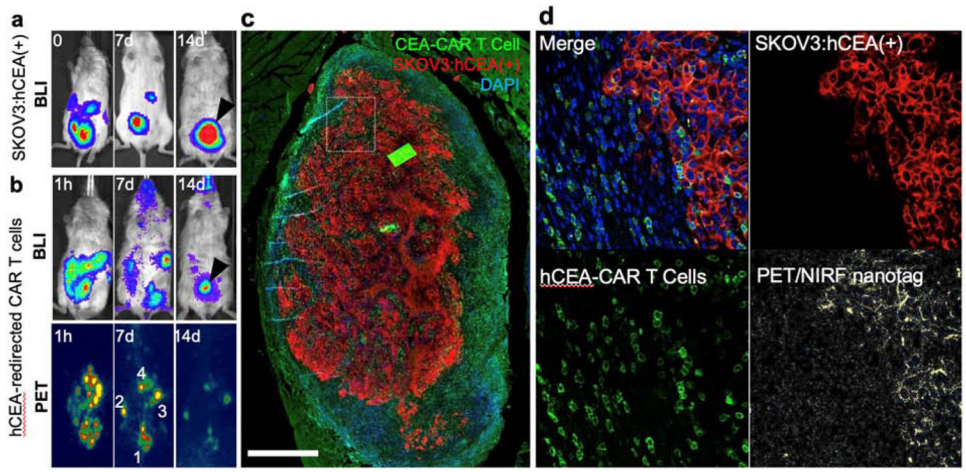

Figure 5. CAR T cell accumulation at the tumor site.

a, Bioluminescence imaging (BLI) of SKOV3:hCEA(+) in an NSG mouse prior to (t=0) and post adoptive T cell (t=7, 14 days). At t=14 post adoptive cell transfer one major lesion was present (arrow head) **b,** BLI and PET imaging at 1 h, 14 days post adoptive cell transfer (i.p.) administration of PET/NIRF nanotag-labeled hCEA-redirected CAR T cells. **c,** Immunofluorescence image of the remaining tumor (red) demonstrates that the majority of CAR T cells (green) were found most prominently in the tumor periphery (scale bar, 1000 μm). **d,** In another section (box) of the tumor it was found that at t=14 days (p.i.) the PET/NIRF nanotags (yellow) are no longer associated with the hCEA-redirected CAR T cells, but have been released and subsequently taken up by the SKOV3:hCEA(+) cancer cells (scale bars, 100 μm)